



Performance Evaluation of Integrated Antennas on Photovoltaic Solar Cells

Ahmed Al-Alawi* , Said Al-Gheilani, Ahmed Al-Zeidi, Mohammed M. Bait-Suwailam 

Dept. of ECE, Sultan Qaboos University, Muscat, Oman, PC-123

*Corresponding author Email: msuwailam@squ.edu.om

HIGHLIGHTS

- The examined antenna performed well when placed in the middle of PV solar cell with a 2.58 dBi peak gain.
- Creating a small air gap between the antenna and the PV solar cell results in better performance.
- The antenna has satisfactory performance when integrated with PV cells.

ARTICLE INFO

Handling editor: Ivan A. Hashim

Keywords:

Antenna; patch antenna; photovoltaic; smart grid; solar cells.

ABSTRACT

The performance of antennas is critical to ensuring reliable wireless communication and robust data transmission. Unfortunately, antennas' performance gets degraded when loaded with lossy materials. This paper presents the numerical and experimental evaluation of low-profile antennas' performance when integrated with photovoltaic (PV) solar cells for potential use in smart grid and green power networks. Such integrated antennas can serve as a communication unit and sensors to monitor PV solar cells. For convenience, a microstrip patch antenna was used in this assessment study, where the antenna was designed, numerically simulated, and experimentally tested. After which, it was installed on top of a PV solar cell at different orientations. The antenna is designed to operate within the 2.45 GHz ISM band. Based on the results, the antenna performed well when placed at the middle of the PV solar cell with a peak gain of 2.58 dBi compared to other placements within the PV solar cell. Moreover, creating a small air gap between the antenna and the PV solar cell results in better performance. Based on the findings of this study, the antenna has satisfactory performance when integrated with PV cells, which is promising to deploy in many applications, including smart grid networks.

1. Introduction

Fossil fuels, such as oil and natural gases, are now widely regarded as one of the major issues affecting the environment worldwide. Significant amounts of CO₂, a greenhouse gas, are released into the atmosphere because of burning fossil fuel as a source of energy. The dramatic rise of using greenhouse gases will lead to increased global warming, which will increase the temperature and sea level on the planet [1]. Renewable energy sources such as solar systems are becoming attractive sources that can be used in power production. To enhance the wireless connectivity of smart grid networks, antennas are widely used for wireless communication applications, for instance, sending real-time data from remote areas to dispatch centers [2, 3].

There has been a renewed interest in designing and integrating antennas with PV solar cells for many engineering applications, including real-time monitoring of PV cells, data transmission/reception from renewable power plants to dispatch centers, and vice versa. The integration seems attractive in terms of cost and design complexity. Ahmed et al. developed a copper indium gallium selenide (CIGS) based solar cell integrated antenna [4]. A highly low-profile integrated antenna was created when the solar cell was cut through. When the solar cell meets this small hole, the clearance area is so tight that the total device size must be raised to compensate. Therefore, a tiny slot antenna was built utilizing lumped components following a ground-radiation antenna design technique. Figure 1 depicts the adopted design.

Another study in [5] incorporated a PV solar cell as an antenna element for GPS signal reception. The proposed antenna structure is shown in Figure 2.

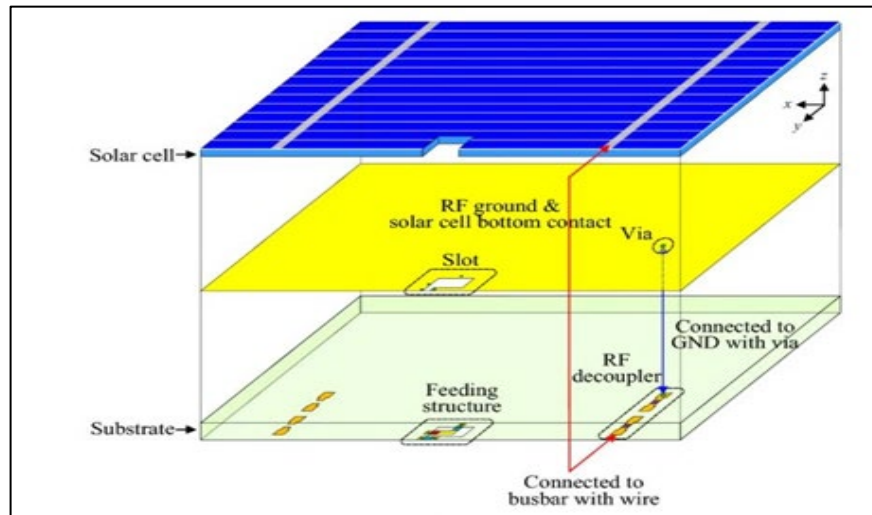


Figure 1: Three-dimensional view of the adopted solar antenna in [2]



Figure 2: The proposed GPS reception antenna system with PV cells [3]

Another interesting research direction related to integrating antennas with PV solar cells is the development of PV solar cell antennas for energy harvesting to recharge low-power wireless devices [6, 7]. The deployment of PV solar cell antennas has also been introduced for many wireless communication applications, including single- and dual-band operations for WLAN [8, 9, 10], and GPS services [11], among others. Recently, space communications have received much interest from academia and industry. One of the potential needs for miniaturization and production of lightweight space crafts is to develop techniques for the potential integration of small antennas with PV solar cells within a combined surface area [12].

Unfortunately, the performance of antennas is degraded when loaded with lossy materials, like PV solar cells. This research aims to investigate the performance of low-profile antenna structures for practical power systems networks and wireless communications needs by testing the optimal location of a low-profile antenna on top of a PV solar cell. In this research paper, we aim to develop antennas with satisfactory performance integrated with solar cells in what is termed integrated antennas for smart grid interconnections. We have carried out numerical and experimental studies on optimal location of microstrip patch antenna (chosen for convenience) as well as developing another alternative to enhance the antenna's performance further by adding a small perturbed air gap between the antenna and the PV solar cell.

2. Methodology

The methodology proposed in this research aims to develop and design three-dimensional models based on electromagnetic simulations. The main focus is on integrating highly radiative antennas with PV solar cells technology to help install such configurations in smart grid networks for wireless communication or even re-charging purposes of sensors. Furthermore, the methodology focuses on fabricating the proposed hybrid antenna system, where the antenna is fabricated using printed circuit board technology.

For convenience, a microstrip inset-fed patch antenna was designed and simulated alone before integration. Note that the antenna was designed to resonate at the 2.45 GHz (ISM-band). The host material of the antenna was selected based on the availability of materials in the laboratory. The antenna's substrate is FR-4 laminate, with a dielectric constant of 4.4 and a loss

tangent of 0.02. It is then much more convenient to design the microstrip patch antenna based on the given dielectric properties of the substrate. The width and length of the patch antenna can be calculated using the following relations [13]:

$$W = \frac{c}{2f} \sqrt{\frac{2}{\epsilon_r + 1}} \tag{1}$$

$$L = L_{eff} - 2\Delta L \tag{2}$$

W and L are the width and length of the patch antenna (in meters), respectively. c is the speed of light (3×10^8 m/s). f is the antenna's resonance frequency (2.45 GHz here). ϵ_r is the relative permittivity of the host material, and L_{eff} is the length accounted for the fringing electromagnetic fields within the patch edges. ΔL is defined below [13]:

$$L_{eff} = \frac{c}{2f\sqrt{\epsilon_{r,eff}}} \tag{3}$$

$$\Delta L = 0.412 * h \frac{(\epsilon_{r,eff} + 0.3) \left(\frac{W}{h} + 0.264\right)}{(\epsilon_{r,eff} - 0.258) \left(\frac{W}{h} + 0.8\right)} \tag{4}$$

And lastly, the effective dielectric constant $\epsilon_{r,eff}$ is defined as [13]:

$$\epsilon_{r,eff} = \frac{\epsilon_r + 1}{2} + \frac{\epsilon_r - 1}{2} \left[1 + 12 \frac{h}{W}\right]^{-1} \tag{5}$$

Figure 3 shows the inset-fed microstrip patch antenna with its structural dimensions. The width and length of the two insets within the patch radiator are designed for a 50-ohm power excitation.

The antenna is then conveniently placed on top of a modeled PV solar cell as an insulating substrate mimicking the response of a silicon-based PV cell. Note that no spacing was placed between the antenna and the PV cell. Figure 4 depicts a top view of the developed integrated antenna structure with PV solar cells using the Finite-Element solver of High-Frequency Simulation Software (HFSS). The antenna and the PV cell dimensions can be found in Table 1.

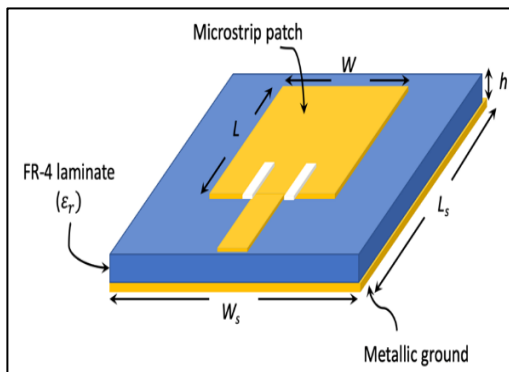


Figure 3: 3D view showing the inset-fed microstrip patch antenna with its structural dimensions

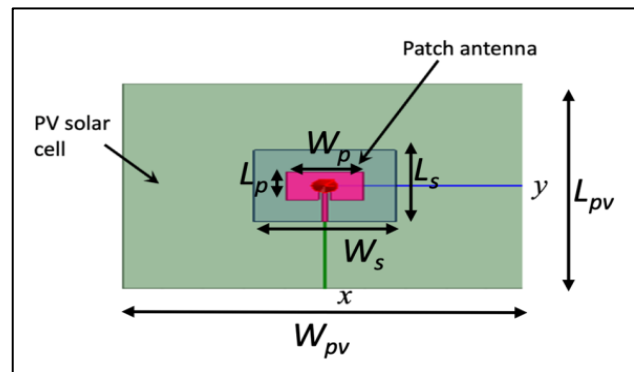


Figure 4: Top view of the microstrip inset-fed patch antenna on top of PV cel

Table 1: Dimensions of the hybrid PV-antenna structure

Parameter(s)	Dimension (in mm)	Parameter(s)	Dimension (in mm)
Patch Length, Lp	28.5	PV cell length, Lpv	320
Patch Width, Wp	38	PV cell width, Wpv	350
Antenna substrate length, Ls	70	PV cell substrate (silicon) thickness	18
Antenna substrate width, Ws	70	Antenna substrate (FR-4) thickness	1.6

A numerical parametric study was carried out to quantify the antenna's performance on top of the PV cell. This numerical study installed the patch antenna in different spots within the PV cell. Figure 5 depicts three scenarios for placing the antenna on top of the PV cell.

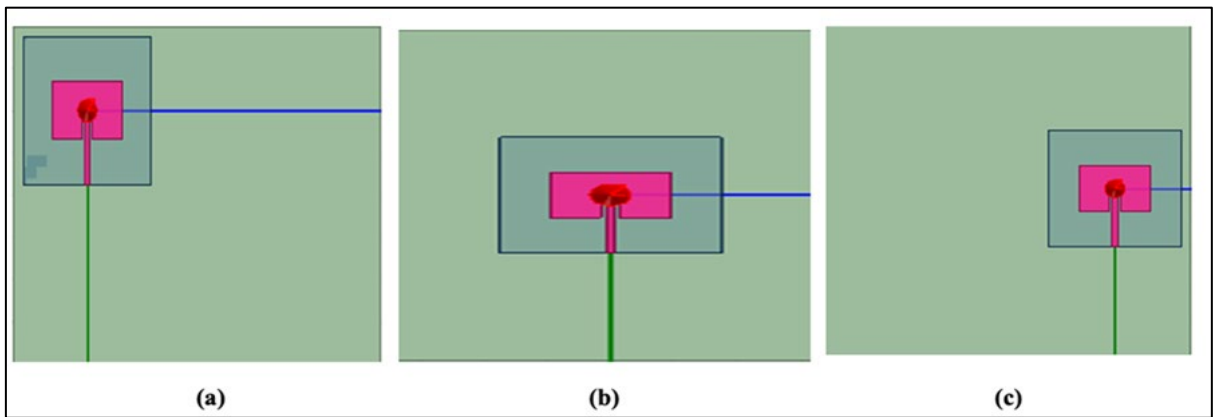


Figure 5: Top view of the microstrip inset-fed patch antenna on top of PV cell, in three different orientations: (a) top left corner; (b) middle of PV cell; and (c) middle right corner

3. Results and Discussions

Figure 6 shows the simulated reflection coefficient for the single-port patch antenna alone, where good matching can be seen within the ISM frequency band.

Next, we present the simulation results for the performance of the inset-fed patch antenna in the middle of the PV solar cell, as shown in Figure 7, where the antenna has a good impedance matching, i.e., < -10 dB, within the 2.4 GHz ISM band

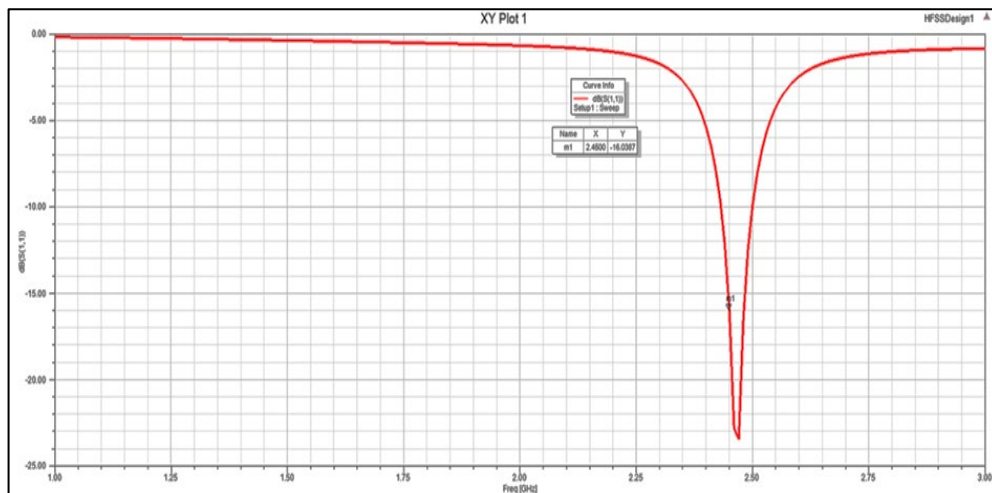


Figure 6: Simulated reflection coefficient of the antenna alone (without PV cell)

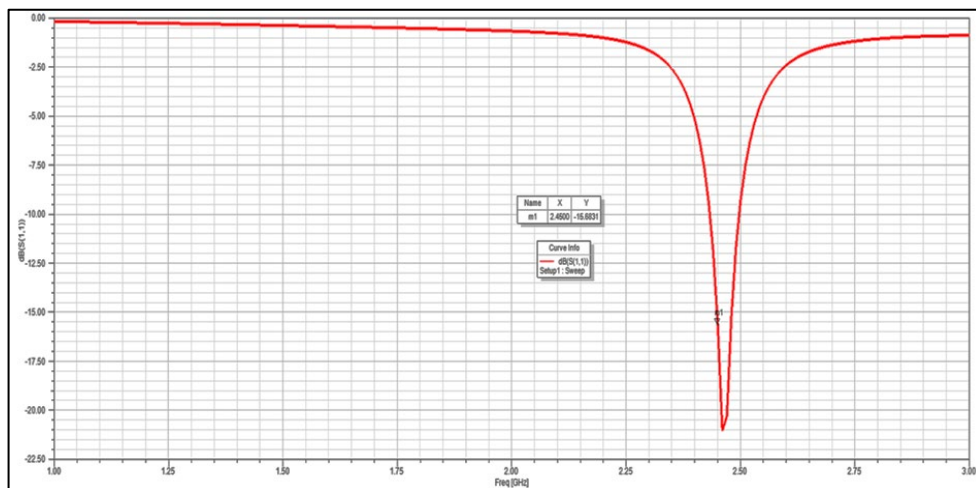


Figure 7: Simulated reflection coefficient of the integrated antenna with PV cell (middle of PV cell)

Table 2 presents the numerical results showing a comparison of the antenna performance on top of the PV cell from the three different orientations. In this parametric study, the antenna was assumed to be touching the PV cell. Thus no air gap is encountered. The antenna's performance was assessed based on its matching impedance, peak gain (in dB), and efficiency (in %). Based on the numerical full-wave electromagnetic simulation results, we can observe that the patch antenna's optimal deployment is placed on top of the PV cell at its middle (center). This is also attributed to minimal effects from fringing fields and backscattered radiation from the edges of the PV cell, thus resulting in a better peak gain. Interestingly, the radiation efficiency of the integrated antenna in the three cases was unaltered.

We have carried out an experimental setup see Figure 8 to quantify the strength of the power received (collected) by the integrated PV-antenna system. In a quasi-controlled laboratory, a horn antenna was used as a transmitter to radiate electromagnetic waves. The three orientation scenarios, as shown in Figure 5, are also considered and compared against the optimal performance of the antenna being alone. Table 3 summarizes the results from this experimental setup, where satisfactory performance was obtained for the three cases of the integrated PV-antennas and comparable to the power received by the microstrip patch antenna alone. This is attributed to the increased footprint area of the antenna structure with a PV cell since the PV solar cell will behave as a reflective layer.

The effect of the air gap embedded as a medium between the antenna and the PV solar cell was also investigated numerically. We have made over 5 parametric sweep data and have observed that the antenna performance can be enhanced further due to the air gap effect. Table 4 presents the antenna's performance on top of the PV solar cell with an intermediate air gap.

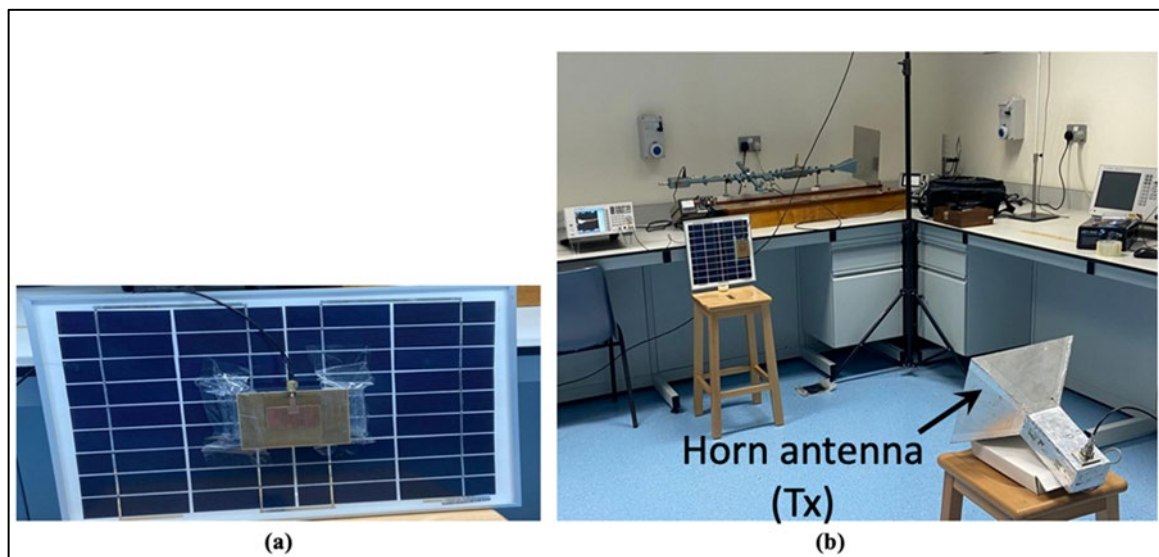


Figure 8: (a) Perspective view of the microstrip inset-fed patch antenna on top of the PV cell; and (b) the experimental setup to measure the power received by the antenna when placed on top of the PV cell

Table 2: The performance of the integrated PV-antenna structure for three different orientations

	At the top-left of the PV cell	At the middle of the PV cell	At the middle-right of the PV cell
S11 (dB)	-14.88	-15.68	-15.45
Peak Gain (dBi)	2.38	2.58	2.08
Radiation efficiency (%)	39	39	39

Table 3: The received power by the integrated PV-antenna structure for three different orientations and compared against the microstrip patch antenna alone

	Antenn a alone	At the top-left of the PV cell	At the middle of the PV cell	At the middle-right of the PV cell
Power received (in dBm)	-20.59	-22.14	-20.16	-20.21

Table 4: The performance of the integrated PV-antenna structure with embedded air-gap

Air gap (mm)	S11 (dB) @ 2.45 GHz	Peak Gain (dBi)	Radiation efficiency (%)
1	-15.74	2.78	40
5	-15.77	3.23	42
10	-15.98	3.45	43
15	-15.79	4.01	44
20	-15.64	4.42	46

At the end of this research work, we present a comparison of previously proposed and developed antenna structures with PV solar cells with our presented work. Table 5 summarizes this short comparison, considering antenna type and some performance metrics, including antenna size. From Table 5, we can see that the performance of our integrated antenna is reasonably acceptable. In the future, we aim to improve further on the integrated antenna performance along with achieving miniaturization.

Table 5: Performance comparison of integrated antennas with PV solar cells in the literature

Reference	Antenna Configuration	Frequency (GHz)	Radiation efficiency (%)	Antenna Size (mm ²)
[9]	PIFA	5.8	97.1	48 × 57
[10]	Slot	2.4/5.2	-	73 × 69
[11]	Patch	1.575	-	350 × 350
[14]	Vivaldi	0.95 – 2.45	70 @ 2.45 GHz	71 × 18
This work	Inset-fed patch	2.45	39 (no air gap) 46 (with air-gap)	× 350

4. Conclusion

This paper investigated numerical and experimental assessment of integrated patch antenna with PV solar cells. The developed integrated antenna structure was first designed and simulated using HFSS software and then fabricated and tested in a quasi-controlled laboratory.

Based on the numerical and experimental results, satisfactory performance of the inset-fed patch antenna on top of a PV solar cell was achieved in terms of far-field parameters along with power collected by the integrated structure. Therefore, it is believed that the integrated PV-antenna structure could be useful in many applications, including smart grid networks and monitoring of PV solar cells' performance. In future studies, we aim to implement the integrated antenna system with PV solar cells as part of a smart grid interconnected network for performance evaluation. From such field trials, we shall improve and develop more innovative antenna solutions for integration with PV solar cells.

Author contribution

All authors contributed equally to this work.

Funding

This research received no specific grant from any funding agency in the public, commercial, or not-for-profit sectors.

Data availability statement

The data that support the findings of this study are available on request from the corresponding author.

Conflicts of interest

The authors declare that there is no conflict of interest.

References

- [1] S. Shynu, M. Ons, M. Ammann, S. Gallagher, B. Norton, Inset-fed microstrip patch antenna with integrated polycrystalline photovoltaic solar cell, in: 2nd European Conference on Antennas and Propagation Edinburgh, UK, 2007. <https://doi.org/10.1049/ic.2007.1373>
- [2] J. R. Albert, A. Stonier, Design and development of symmetrical super-lift DCAC converter using firefly algorithm for solar-photovoltaic applications, IET Circuits Devices Syst., 14 (2020) 261–269. <https://doi.org/10.1049/iet-cds.2018.5292>
- [3] J. R. Albert, et al., Investigation on load harmonic reduction through solar-power utilization in intermittent SSFI using particle swarm, genetic, and modified firefly optimization algorithms, J. Intell. Fuzzy Syst: Appl. Eng. Technol., 42 (2022) 4117–4133. <https://doi.org/10.3233/jifs-212559>
- [4] A. Ali, H. Wang, J. Lee, Y. H. Ahn, I. Park, Ultra-low profile solar-cell-integrated antenna with a high form factor, Sci. Rep., 11 (2021) 20918. <https://doi.org/10.1038/s41598-021-00461-w>
- [5] A. S. Kumar, S. Sundaravadivelu, An efficient design of solar cell antenna for mobile and vehicular applications, in: 2011 IEEE Global Humanitarian Technology Conference, Seattle, WA, USA, 2011, 36-39. <https://doi.org/10.1109/ghtc.2011.14>
- [6] C. Baccouch, H. Sakai, D. Bouchouicha, T. Aguila, Leaf-shaped solar cell antenna for Energy Harvesting and RF Transmission in KU-band, Adv. Sci. Technol. Eng. Syst. J., 2 (2017) 130–135. <https://doi.org/10.25046/aj020616>
- [7] O. O'Conchubhair, P. McEvoy, M. Ammann, Integration of antennas array with multicrystalline silicon solar cell, IEEE Antennas Wirel. Propag. Lett., 14 (2015) 1231-1234. <https://doi.org/10.1109/lawp.2015.2399652>

- [8] C.-Y.-D. Sim, C.-C. Chen, X. Y. Zhang, Y.-L. Lee, C.-Y. Chiang, Very small-size uniplanar printed monopole antenna for dual-band WLAN laptop computer applications, *IEEE Trans. Antennas Propagation*, 65 (2017) 2916–2922. <https://doi.org/10.1109/tap.2017.2695528>
- [9] O. Yurduseven, D. Smith, A solar cell stacked multi-slot quadband PIFA for GSM, WLAN and WiMAX networks, *IEEE Microwave Wireless Compon. Lett.*, 23 (2013) 285–287. <https://doi.org/10.1109/lmwc.2013.2258006>
- [10] S. V. Shynu, M. J. R. Ons, M. J. Ammann, S. J. McCormack, B. Norton, Dual band a-Si:H solar-slot antenna for 2.4/5.2 GHz WLAN applications, 2009 3rd European Conference on Antennas and Propagation, Berlin, Germany, 2009, 408-410.
- [11] N. Henze, A. Giere, H. Fruchting, GPS patch antenna with photovoltaic solar cells for vehicular applications, 2003 IEEE 58th Vehicular Technology Conference. VTC 2003-Fall (IEEE Cat. No.03CH37484), Orlando, FL, USA, 1, 2003, 50-54. <https://doi.org/10.1109/vetecf.2003.1284976>
- [12] J. Huang, M. Zawadzki, Antennas integrated with solar arrays for space vehicle applications, 2000 5th International Symposium on Antennas, Propagation, and EM Theory. ISAPE 2000 (IEEE Cat. No.00EX417), Beijing, China, 2000, 86-89. <https://doi.org/10.1109/isape.2000.894730>
- [13] Balanis, C.A. *Antenna Theory: Analysis and Design*, 3rd Edition, John Wiley & Sons, Inc., 2005.
- [14] O. O’Conchubhair, K. Yang, P. Mcevoy, Amorphous silicon solar vivaldi antenna, *IEEE Antennas Wirel. Propag. Lett.*, 15 (2016) 893–896. <https://doi.org/10.1109/LAWP.2015.2479189>